Carbohydrate Polymers 78 (2009) 349–356

Contents lists available at ScienceDirect

Carbohydrate Polymers

journal homepage: www.elsevier.com/locate/carbpol

Effects of the cooling mode on the structure and strength of porous scaffolds made of chitosan, alginate, and carboxymethyl cellulose by the freeze-gelation method

Nai-Yi Yuan [a], Yi-An Lin [a], Ming-Hwa Ho [b], Da-Ming Wang [a], Juin-Yih Lai [c], Hsyue-Jen Hsieh [a,*]

[a] Department of Chemical Engineering, National Taiwan University, Taipei 10617, Taiwan
[b] Department of Chemical Engineering, National Taiwan University of Science and Technology, Taipei 10607, Taiwan
[c] Research and Development Center for Membrane Technology, Chung Yuan University, Chung-Li, Taoyuan 32023, Taiwan

ARTICLE INFO

Article history:
Received 17 February 2009
Received in revised form 15 April 2009
Accepted 20 April 2009
Available online 3 May 2009

Keywords:
Mechanical properties
Supercooling
Polysaccharide
Scaffold
Freeze-gelation

ABSTRACT

A freeze-gelation method was utilized to prepare porous scaffolds made of chitosan, alginate, and carboxymethyl cellulose because of their usefulness in tissue engineering applications. These polysaccharide solutions were cooled down to freezing using either a fast-cooling (FC) mode (>20 °C/min) or a slow-cooling (SC) mode (0.83 °C/min). Then the frozen polysaccharide solutions were immersed in their respective non-solvents to form porous scaffolds. Based on the SEM and optical microscope images of the scaffolds, the FC mode induced non-simultaneous nucleation and generated directional pore structures. In contrast, simultaneous nucleation and uniform and isotropic pore structures (mean pore size: 60–100 μm) were obtained by using the SC mode. Moreover, the tensile strength of the scaffolds prepared by the SC mode (about 60 N/g) was three times higher than that of scaffolds prepared by the FC mode (about 20 N/g). This study reveals that when using the freeze-gelation method, the cooling rate (mode) is a crucial factor which controls the pore structure and strength of porous scaffolds. Therefore, our results suggest that polysaccharide scaffolds with pore structures suitable for tissue engineering applications can be obtained via an appropriate cooling mode.

1. Introduction

Polysaccharides are extensively used in tissue engineering (Kim et al., 2008) and drug delivery systems (Dong & Leong, 2006; George & Abraham, 2006) because of their numerous beneficial biological properties (Muzzarelli et al., 1988). Porous polysaccharide scaffolds are able to provide three-dimensional structures for both in vitro studies of cell–scaffold interactions as well as in vivo studies of induced tissue regeneration (Dong & Leong, 2006; Kim et al., 2008; Ma et al., 2003). High porosity (generally greater than 90%) and a large pore size (about 100 μm) as well as an interconnected pore structure of the porous scaffolds are necessary for the transport of cells and metabolites (Rezwan, Chen, Blaker, & Boccaccini, 2006). Previous reports showed that adhesion, proliferation, and phenotype of cells were affected by the pore size distribution and pore shape of scaffolds (Berry, Campbell, Spadiccino, Robertson, & Curtis, 2004; Zeltinger, Sherwood, Graham, Müeller, & Griffith, 2001).

A freeze-gelation method was developed by Ho et al. for fabricating porous scaffolds for tissue engineering applications (Ho et al., 2004). Their method is based on thermally induced phase separation (TIPS) (Nam & Park, 1999; Whang, Thomas, Healy, & Nuber, 1995) and immersion precipitation. In the freezing step (TIPS), a homogeneous aqueous polymer solution is frozen in a cooling process to induce liquid–liquid demixing or solid–liquid demixing. Then, the frozen solution is immersed in a non-solvent of the polymer to remove the frozen solvent, and the polymer forms a porous scaffold. Compared with the freeze-drying method, the freeze-gelation method saves time and energy, and is easier to scale up (Ho et al., 2004).

However, in an aqueous polymer solution, the presence of polymer molecules may affect the equilibrium and non-equilibrium properties of the water as ice crystals are generated during the freezing process. A wide range of melting (T_m) and freezing temperatures (T_f) reflects the non-ideal behavior of the solution at high concentrations (Koop, Luo, Tsias, & Peter, 2000). At the end of ice solidification, the pore size and structure of the scaffolds were determined by the ice-crystal morphology and size distribution (O'Brien et al., 2004). Bigg reported in 1953 that the cooling rate has a dramatic effect on freezing, with significant supercooling possible at high cooling rates (Bigg, 1953; Chen & Lee, 1998). Supercooled water is in a metastable state which ends when ice nucleation occurs and ice crystals form. The latent heat released from the ice crystals are consumed by the supercooled water, and the temperature of water returns to its freezing point (0 °C) during the growth process of the ice crystals. It was observed that the freezing temperature decreased with the cooling rate up to a

* Corresponding author. Tel.: +886 2 23633097; fax: +886 2 23623040.
E-mail address: hjhsieh@ntu.edu.tw (H.-J. Hsieh).

0144-8617/$ - see front matter © 2009 Elsevier Ltd. All rights reserved.
doi:10.1016/j.carbpol.2009.04.021

certain value in deeper supercooled states (Gokhale, 1964). Previous study showed that varying the rate of ice nucleation may result in ice crystals of different morphologies (Wood & Walton, 1970).

A recent study indicated that adjusting the cooling rate can affect phase separation via different ice nucleation mechanisms, resulting in scaffolds with various morphologies of pore sizes and distributions as well as scaffold heterogeneity, thus affecting their mechanical properties (Hollister, 2005). Different scaffold microstructures lead to different effective stiffness levels. A scaffold's mechanical properties (strength, toughness, and ductility) are determined both by properties of the bulk material such as the material chemistry and by its structure such as the material/pore arrangement (Muschler, Nakamoto, & Griffith, 2004). For porous scaffolds prepared by the freeze-drying method using different freezing temperatures, it was reported that a lower freezing temperature can induce smaller pore sizes (Kuo & Ku, 2007; Moshfeghian, Tillman, & Madihally, 2006). In our previous research, we found that using an elevated pre-cooled bath temperature and concentration of acetic acid, the tensile stress and strain of the chitosan scaffolds at maximum load significantly increased (Hsieh et al., 2007). However, the effects of the cooling rate on the mechanical properties and pore structure of scaffolds have not been extensively investigated. In order to demonstrate that the cooling rate is an important factor that affects the properties of porous scaffolds, three polysaccharides, chitosan (CH), alginate (AL), and carboxymethyl cellulose (CMC), were used to prepare porous scaffolds by the freeze-gelation method, and the characteristics of the scaffolds were determined. CH, AL, and CMC are often used for tissue engineering applications and also drug release systems (Faroongsarng & Sukonrat, 2008; George & Abraham, 2006; Kim et al., 2008; Kokini & Surmay, 1994; Wang, Kao, & Hsieh, 2003).

As to the nature of the material, CH is a copolymer of glucosamine and *N*-acetylglucosamine which is generally obtained from crustacean shells and cell walls of fungi (Muzzarelli et al., 1988; Wang et al., 2003). AL is a linear unbranched polymer containing β-(1,4)-linked D-mannuronic acid and α-(1,4)-linked L-guluronic acid residues (George & Abraham, 2006; Kokini & Surmay, 1994), whereas CMC is a cellulose derivative with carboxymethyl groups ($-CH_2-COOH$) bound to some of the hydroxyl groups of the glucopyranose repeating units which have different degrees of substitution, but it is generally in the range of 0.6–0.95 derivative per repeating unit (Capitania, Porrob, & Segre, 2000). It is noteworthy that ethanol is a non-solvent of CH, AL, and CMC for immersion precipitation in the freeze-gelation method.

The aim of this study was to investigate the influence of cooling rate (mode) on the final characteristics of the porous polysaccharide (CH, AL, and CMC) scaffolds fabricated by the freeze-gelation method. Ice nucleation phenomena under different cooling rates were compared to better understand how the cooling rate affects the pore structure and tensile strength of the porous scaffolds, which were assessed by scanning electron microscope (SEM), optical microscope and mechanical strength analysis.

2. Experimental

2.1. Materials

Chitosan (CH, M_W = 300,000, degree of deacetylation = 85–90%) was obtained from Kiotek (Hsinchu, Taiwan). Alginate sodium salt (AL, from the kelp *Macrocystis pyrifera*), and carboxymethyl cellulose sodium salt (CMC, medium viscosity of 400–800 cps in a 2% aqueous solution at 25 °C) were purchased from Sigma–Aldrich (St. Louis, MO, USA). All solvents used were of analytical quality. Distilled and deionized water was used throughout this study. Other chemicals were purchased from Sigma–Aldrich.

2.2. Preparation of polysaccharide aqueous solutions

CH powder and water were poured into a bottle which was covered with insulated materials (FANYALON® NP-620, Fanyalon, Taichung Hsien, Taiwan) to avoid heat exchange with the surroundings (insulated system). Then, acetic acid was added to the system to dissolve the CH and form a 3-wt% chitosan 0.2 M acetic acid aqueous solution. During the dissolution process, the temperature profile with respect to time was measured by a T-type thermocouple (TP-K02, TES Corp., Taipei, Taiwan) and recorded with a digital thermometer (TES-1307, TES). Data were transmitted to a computer for further analysis. AL and CMC were directly dissolved in pure water to form a 3-wt% aqueous solution. In addition, the apparent viscosities of the three polysaccharide aqueous solutions were determined by a viscometer (model DV-II+, Brookfield, Middleboro, MA, USA).

2.3. Preparation of the polysaccharide scaffolds

The polysaccharide scaffolds were prepared by a freeze-gelation method developed by Ho et al. (2004). A diagram of the experimental apparatus is shown in Fig. 1a. It consists of a mold section and a cooling section. The mold section, as shown in Fig. 1b, contains a homemade acrylic square frame that was divided into 10 hollow areas. Each hollow area is a cuboid with a length of 8 cm, a width of 2.5 cm, and thickness of 0.3 cm. The 3 wt% polysaccharide solution (about 60 g) was enclosed in the acrylic frame, and placed between two stainless steel plates (15 × 15 × 0.3 cm) (at the top and bottom for heat exchange) to form a sandwich-like mold. Afterwards, the mold was put into a refrigerated bath circu-

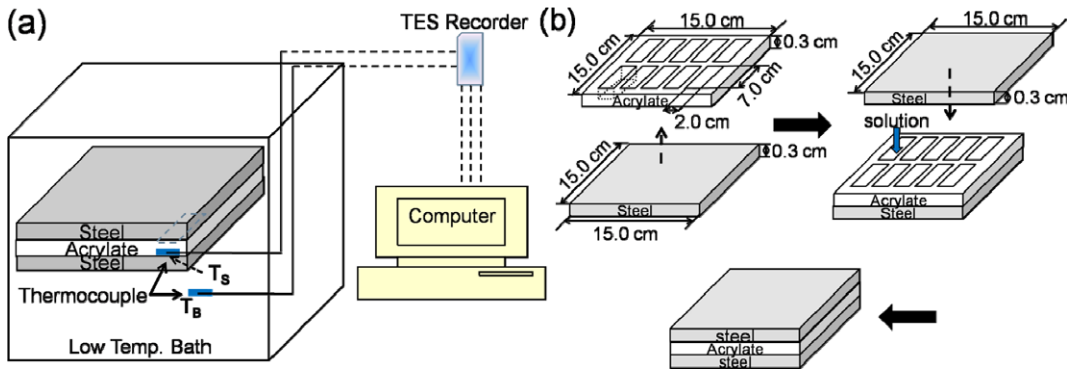

Fig. 1. Schematic diagram of the experimental apparatus: (a) cooling section and (b) mold section. The local temperatures of the polysaccharide solution (T_S) and bath (T_B) were measured.

lator (the cooling section, model BL-80, TIT Co., Taipei, Taiwan) for cooling. Two kinds of cooling modes were used and are described as follows.

Fast-cooling (FC) mode: The prepared mold was quenched in a pre-cooled bath with different bath temperatures (T_B) of −20, −40, −60, or −80 °C. Different temperature gradients were generated in the initial quenching step that induced different FC rates.

Slow-cooling (SC) mode: The mold was cooled in a cooling bath at a constant cooling rate of 0.83 °C/min from 20 °C to final bath temperatures (T_B) of −20, −40, −60, and −80 °C. The rate of cooling was controlled by an RTD temperature controller.

During the cooling processes (FC and SC), temperatures of the solutions (T_S) in the mold and bath temperatures (T_B) were measured using a T-type thermocouple. The data were recorded and analyzed on a notebook computer. The entire cooling process lasted at least 150 min until the temperature reached the final bath temperature, and then the frozen polysaccharide solution was taken out of the mold and immersed in different non-solvents at −20 °C for 3 h to precipitate different polysaccharides, thus forming the porous scaffolds. The non-solvent of CH was a NaOH/ethanol aqueous solution (pH 13), and the non-solvent of CMC was an HCl/ethanol aqueous solution (pH 2.2), because CH and CMC were precipitated at different pH values. To stabilize the AL scaffolds, a $CaCl_2$/ethanol aqueous solution (the concentration of $CaCl_2$ solution was 1 wt%) was chosen to be the non-solvent of AL. Afterwards, all scaffolds were immersed in another non-solvent bath (a 95% ethanol aqueous solution) at −20 °C for 3 h. Finally, the CH scaffold was washed with a phosphate-buffered saline (PBS) solution, and the AL and CMC scaffolds were washed with a 70% ethanol aqueous solution three times (30 min each time) at 25 °C. The scaffolds were dehydrated step-wise in an ethanol solution starting at 70% and continuing to 100% (70%, 80%, 90%, 95%, and 100%) for approximately 15 min in each step. Afterwards, the scaffolds were dried in a Tousimis PVT-3D critical point dryer (Rockville, MD, USA). All scaffolds were stored at 4 °C for further use.

2.4. Evaluation of scaffold porosity

The porosity of a porous scaffold was evaluated as follows:

$$\text{Porosity } (\%) = \left(1 - \frac{V_{\text{polysaccharide}}}{V_{\text{scaffold}}}\right) \times 100\% = \left(1 - \frac{W_{\text{scaffold}}}{\rho_p \times l \times A}\right) \times 100\%,$$

where V_{scaffold} and $V_{\text{polysaccharide}}$ are the volume of scaffold and that occupied by the polysaccharide, respectively, ρ_p is the intrinsic density of the polysaccharide (1.342 g/cm^3 for CH (Thomson et al., 1999), 2.64 g/cm^3 for AL, and 1.59 g/cm^3 for CMC). The area (A), mass (W_{scaffold}), and thickness (l) of the scaffold were measured and used to estimate the overall porosity of the scaffold using the above equation.

2.5. Observation of the scaffold structures

To observe the structures of the scaffolds with a scanning electron microscope (SEM), the scaffolds were dehydrated step-wise in an ethanol solution starting at 70% and continuing to 100% for approximately 15 min for each step. Afterwards, the scaffolds were dried in a Tousimis PVT-3D critical point dryer (Rockville, MD, USA), sectioned, sputter-coated with gold in a Hitachi JEOL JFC-1100E and JEOL JEE-4X vacuum evaporator (Tokyo, Japan), and then visualized using a Hitachi JSM-6300 scanning electron microscope. For observation of the solidified polysaccharide solutions with an optical microscope, CH was stained with a Crocein Orange G dye solution (1 μg/ml), and AL and CMC were stained with a crystal violet solution (1 μg/ml). The frozen polysaccharide solutions prepared by either the SC or FC mode with a T_B of −20 °C without immersion in a non-solvent were maintained at a low temperature and observed with an Olympus inverted microscope (Tokyo, Japan) equipped with a charge coupled device (CCD) image collection system connected to a personal computer.

2.6. Determination of the mechanical properties of the scaffolds

The tensile strength and elongation at maximum load of the porous scaffolds were determined using a Lloyd LRX tensile strength instrument (Hampshire, UK) at a constant speed of 10 mm/min with a preload of 0.1 N. Samples were cut into a typical dog-bone shape similar to the American Society for Testing Material (ASTM) D 4762-04 standard, and then each sample was weighed. The thickness of each individual scaffold was measured. The measured maximum tensile strength (load to fracture) was normalized by weight for each scaffold.

2.7. X-ray diffraction (XRD)

XRD was used to characterize the crystal structure of the scaffolds, which is related to the mechanical strength. The XRD patterns were determined using an X-ray diffractometer (Philips X'Pert MPD Pro, PANalytical, Westborough, MA, USA) and Cu K radiation with a voltage of 45 kV and an intensity of 40 mA. The crystal structures of the polysaccharide scaffolds prepared by the freeze-gelation method with either the FC or SC mode to T_B of −80 °C were examined by measuring the X-ray powder diffraction patterns. The data were collected over a 2θ angular range of 15–50° in a continuous mode with a scan rate of 0.5°/min, and then the X-ray diffractograms were analyzed.

2.8. Statistical analysis

The statistical analysis was performed using the one-way analysis of variance (ANOVA) method (SPSS 14.0, SPSS Taiwan Corp., Taipei, Taiwan) to determine whether differences in the data were significant. Data are expressed as the mean ± standard deviation (SD) ($n \geqslant 5$), and differences were considered statistically significant if $p < .05$.

3. Results and discussion

3.1. Dissolution of chitosan

The dissolution process involves three steps, all of which include a change in enthalpy (Perkyns & Pettitt, 1996). The first step is an endothermic process in which solvent molecules overcome attractive forces in the solute particles such as lattice energy of crystalline materials. The second step is also an endothermic process which involves the separation of solvent molecules to accommodate the solute. The final step is the formation of new attractive interactions between solvent and solute molecules and is exothermic. The sum of the enthalpy change for all three steps determines whether the overall dissolution process is endothermic or exothermic. Since chitosan is a semi-crystalline polymer, lattice energy is released during the dissolution process. However, the temperature increase during the dissolution process of chitosan revealed that it is an exothermic process. That is to say, the energy of the attractive interaction between CH and the acetic acid aqueous solution was greater in magnitude than the lattice energy of CH. Based on our experimental data, the overall heat release for the CH dissolution process can be evaluated as follows:

$$[(M_W \times C_{PW} + M_B \times C_{PB}) \times \Delta T] \fallingdotseq [(100\ g \times 4.18\ J/g\ K + 217.9\ g \times 0.84\ J/g\ K) \times 3.8\ K] = 2283\ J,$$

where M_W and M_B are the respective weights of water and the glass bottle, C_{PW} and C_{PB} are the heat capacities of water and the glass bottle, respectively, and ΔT is the temperature change (increase) during the dissolution process. The above experimental data indicates that the dissolution process of chitosan is exothermic, and thus the phase-separation of CH from its solvent ought to be endothermic during the freezing-induced phase separation step in the fabrication of CH scaffolds. However, in our experiment the total mass of CH in the solution was only 3 g, and there was 95.8 g of water in the solution. The total energy change of CH dissolution was about 2283 J which is quite small compared to the total latent heat of solidification of water (95.8 g × 334.4 J/g = 32035 J, where 334.4 J/g is heat of solidification of water per gram), but it still had a significant effect on the phase-separation process of the CH aqueous solution.

Table 1
Freezing temperature (T_f), initial cooling rate, and the time required for freezing to begin of the polysaccharide solutions using the fast-cooling (FC) mode with different bath temperatures (T_B) ($n \geqslant 3$, mean ± *SD*).

Polysaccharide	T_B (°C)	T_f (°C)	Initial cooling rate (°C/min)	Time required for freezing to begin (s)
Chitosan (CH)	−20	−1.6 ± 1.0	27.9 ± 1.0	150 ± 37
	−40	−2.5 ± 2.2	37.1 ± 1.8	109 ± 14
	−60	−5.1 ± 4.8	48.8 ± 2.5	71 ± 6
	−80	−6.5 ± 6.0	59.8 ± 3.9	52 ± 13
Alginate (AL)	−20	−0.2 ± 1.7	26.7 ± 4.0	150 ± 28
	−40	−1.2 ± 2.8	35.8 ± 6.2	51 ± 21
	−60	−3.5 ± 3.1	49.5 ± 8.4	33 ± 10
	−80	−5.2 ± 3.5	58.8 ± 10.5	22 ± 10
Carboxymethyl cellulose (CMC)	−20	−3.2 ± 2.8	24.4 ± 1.2	143 ± 40
	−40	−4.6 ± 3.3	31.2 ± 2.5	100 ± 13
	−60	−6.2 ± 4.5	42.5 ± 3.2	84 ± 10
	−80	−8.5 ± 5.5	55.5 ± 4.1	56 ± 12

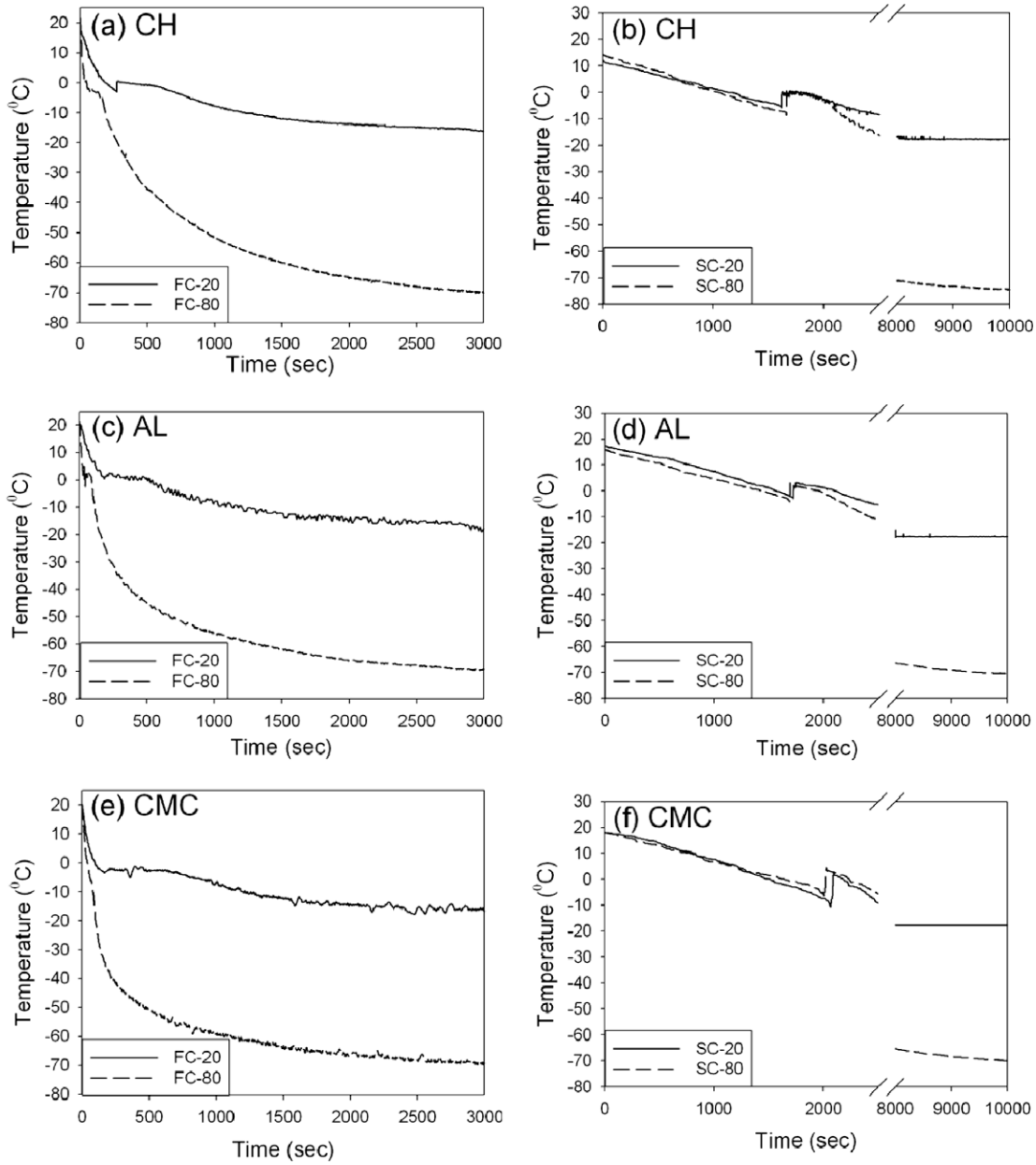

Fig. 2. Time course of solution temperature (T_S) under fast-cooling (quenching, FC) mode and slow-cooling (at a cooling rate of 0.83 °C/min, SC) mode with different final bath temperatures (T_B) (−20 and −80 °C). (a and b) Chitosan (CH), (c and d) alginate (AL), and (e and f) carboxymethyl cellulose (CMC).

3.2. Temperature profile of the cooling modes

The freezing step in the freeze-gelation method was carried out by either the FC or SC mode. Heat transfer in the cooling process is associated with heat conduction and natural convection, and the phase-separation process includes ice nucleation and solidification. For the FC mode, the temperature profiles of different polysaccharide solutions with various T_B values are shown in Fig. 2. Since the process of separation of the polymer from the solution can be endothermic or exothermic, the change in temperature became complicated. The entire cooling process can be divided into three stages: solution sensible cooling stage, phase-separation stage (including ice nucleation and solidification), and frozen solution sensible cooling stage. During the solution sensible cooling stage, heat conduction and natural convection are the dominative heat transfer mechanisms (Chen & Lee, 1998; Yoon et al., 2001; Zhang et al., 2005). In the phase-separation stage, heat transfer by conduction and latent heat released during phase change of water into ice are the principle heat exchange processes. From the temperature curve of the polysaccharide aqueous solution in the FC mode, there was no significant temperature change in the phase-separation stage. This means that the rate of ice nucleation growth was comparatively slow, and is regarded as a non-simultaneous nucleation mechanism. Primary nucleation was the initial ice nucleation event. Secondary nucleation (ice growth) followed primary nucleation, and moved with a velocity on the order of

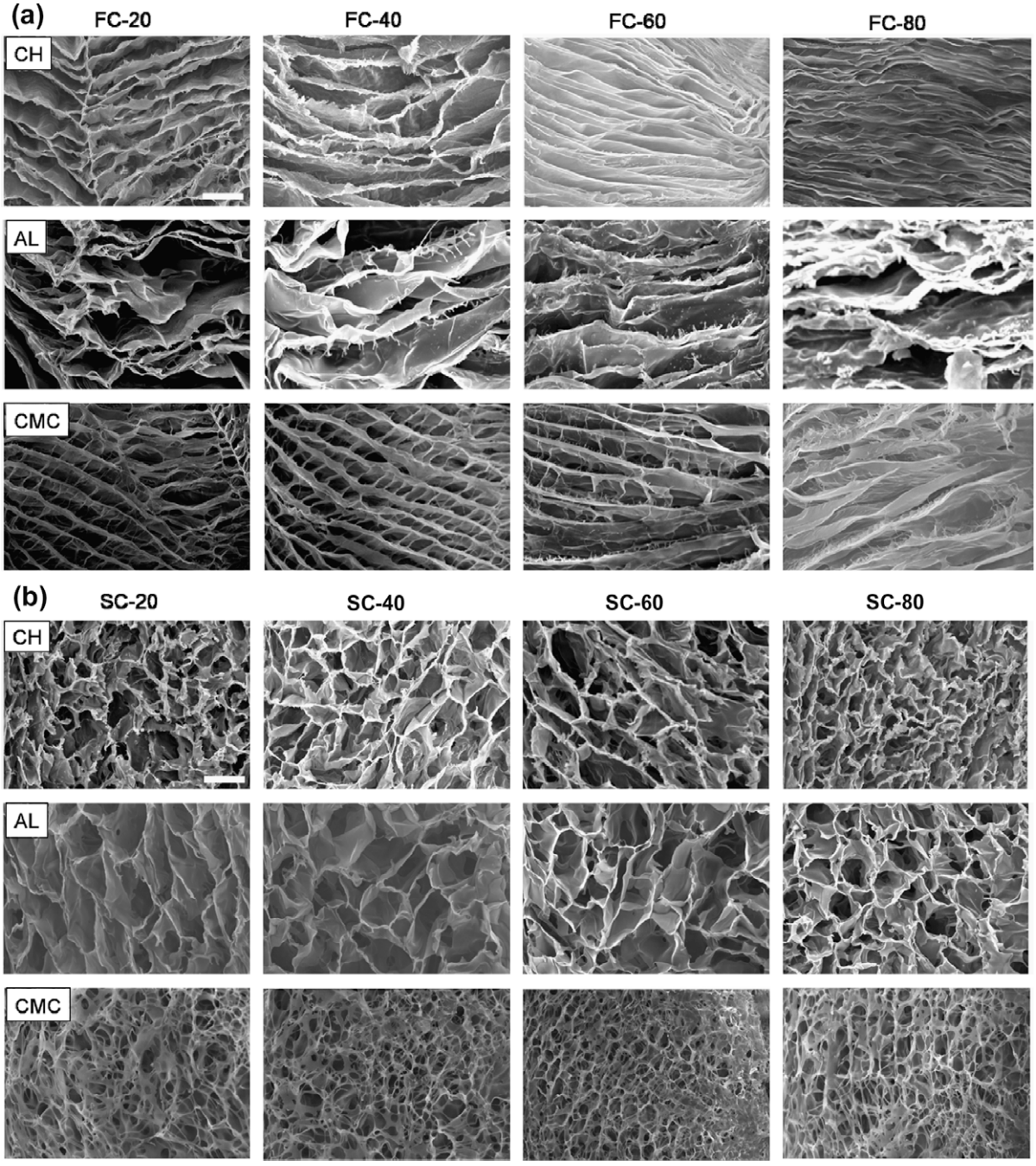

Fig. 3. SEM images of the chitosan (CH), alginate (AL), and carboxymethyl cellulose (CMC) scaffolds prepared by the freeze-gelation method using the (a) fast-cooling (FC) and (b) slow-cooling (SC) mode with different bath temperatures (T_B = −20, −40, −60, and −80 °C). (Bar = 100 μm).

mm/s to the supercooled water region until the solidification process was complete. Secondary nucleation often is referred to as crystallization, and the velocity of solidification is referred to the linear velocity of crystallization (Budiaman & Fennema, 1987).

The average freezing temperature and cooling rate of the FC mode are shown in Table 1. The results demonstrated a wide range of freezing temperatures of the aqueous solution under the high cooling rate condition (Okawa, Saito, & Suto, 2002). In comparing the different polysaccharides, the time required for freezing to begin in the AL aqueous solution was less than those for the CH and CMC aqueous solutions (shown in Table 1). Because the viscosity of the AL (320 cp) solution was less than that of the CH (4460 cp) and CMC (4600 cp) solutions, natural convection was more exuberant for the lower viscosity solution at the same temperature gradient, and it thus increased the speed of eliminating the sensible heat and decreased the time required for freezing to begin. In addition, Tammann reported in 1925 that the velocity of the secondary nucleation front first increases with the extent of supercooling then decreases at deep supercooling due to the effect of high viscosity (Searles, Carpenter, & Randolph, 2001). Therefore, in the FC mode, the high cooling rate induced a large temperature gradient which produced ice crystals generated from the outside to the center of the solution, and directional solidification developed. Ice nucleation first occurred at the surface of the steel, but the latent heat of solidification warmed up the supercooled water, thus decreasing the velocity of ice growth. For all cases of the SC mode with different T_B values, the freezing temperatures were around −5 to −10 °C, and then the temperatures suddenly rose to around the freezing point of water (0 °C) (shown in Fig. 2). This is because of the large amount of latent heat released from the ice crystals, which was simultaneously generated, thus inducing a jump in the solution temperature. Therefore, in the SC mode, simultaneous ice nucleation occurred because as the entire polysaccharide solution was cooled to the same supercooled degree, ice nuclei formed everywhere in the solution and the growth rate of ice crystals increased at the same time (Budiaman & Fennema, 1987; Guzman & Braga, 2005; Okawa et al., 2002).

3.3. Morphology of the scaffolds

The microstructures of the cross-section of the polysaccharide scaffolds are shown in Fig. 3. For the FC mode with a T_B of −20 to −80 °C, stratiform pore structures were observed in the cross-sectional SEM images (Fig. 3a). Because of the presence of large temperature gradients caused by the high cooling rate in one direction during the freezing step in the preparation of the scaffolds, ice crystals grew in one direction which was the same as the direction of the temperature gradient (Zhang et al., 2005). Therefore, at the end of the growth process of ice crystals, a stratiform pore structure had developed.

In contrast, uniform and isotropic pore structures were observed in SEM images of scaffolds produced by the SC mode. Be-

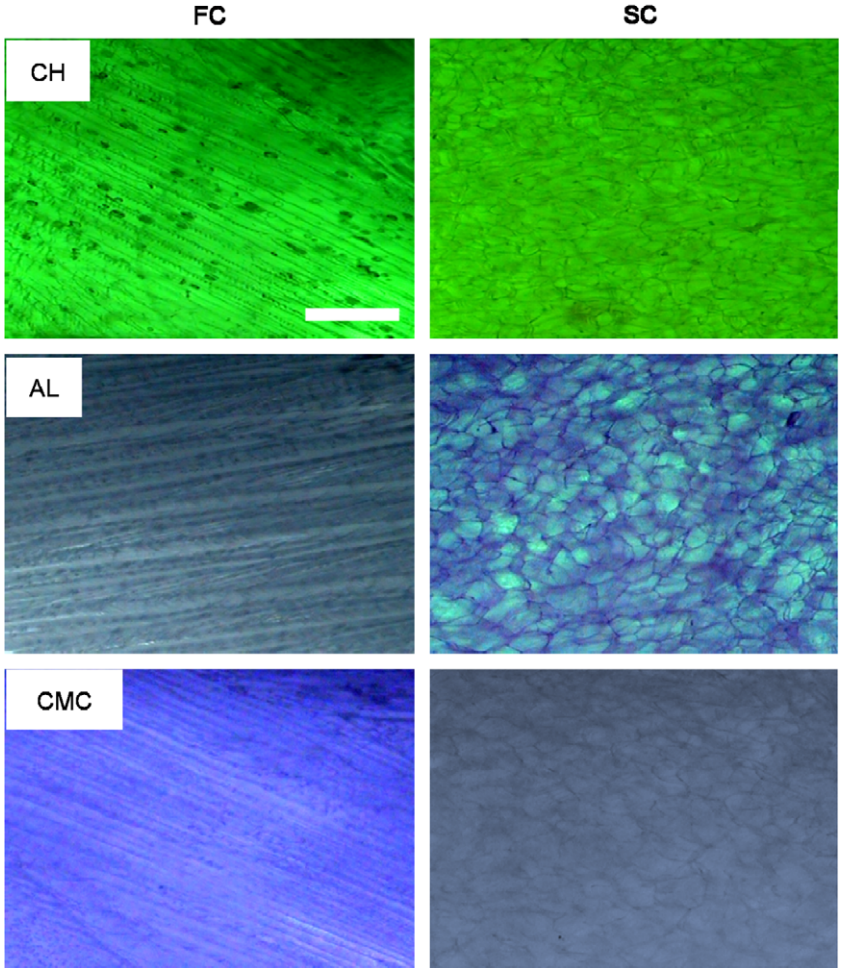

Fig. 4. Optical microscopic images of the chitosan (CH), alginate (AL), and carboxymethyl cellulose (CMC) solutions prepared using the fast-cooling (FC) and slow-cooling (SC) modes (T_B = −20 °C). (Bar = 100 μm).

cause simultaneous nucleation occurred under the SC condition, ice crystals formed throughout polysaccharide solutions at the same time and thus induced isotropic pore structures. The cross-sectional SEM images demonstrated that the pores were interconnected with high porosity.

Optical microscopic photos of the frozen polysaccharide solutions at a T_B of −20 °C are shown in Fig. 4. The patterns of the frozen polysaccharide solutions were similar to the SEM images. An aligned structure of the polysaccharide was observed with the FC mode, but an isotropic structure of the polysaccharide was observed with the SC mode. This indicates that the microstructures of the polysaccharide scaffolds were determined by the freezing-induced phase separation which was affected by the cooling mode. These results are consistent with the inferences discussed in Section 3.2.

3.4. Porosity, mechanical properties, and X-ray diffraction analyses of the scaffolds

All of the scaffolds had high porosities exceeding 96%. That is to say, the cooling rate did not have a significant effect on the porosity of the freeze-gelled porous polysaccharide scaffolds prepared with the same concentration of polysaccharide solution. The mechanical properties of the tensile strength and elongation of the polysaccharide scaffolds with different cooling modes are shown in Fig. 5. The tensile strengths of the CH (Fig. 5a), AL (Fig. 5c), and CMC scaffolds (Fig. 5e) fabricated by the freeze-gelation method with the SC mode were significantly greater than those with the FC mode. Elongation of the CH and CMC scaffolds prepared by the SC mode was higher than that prepared by the FC mode, but there was no

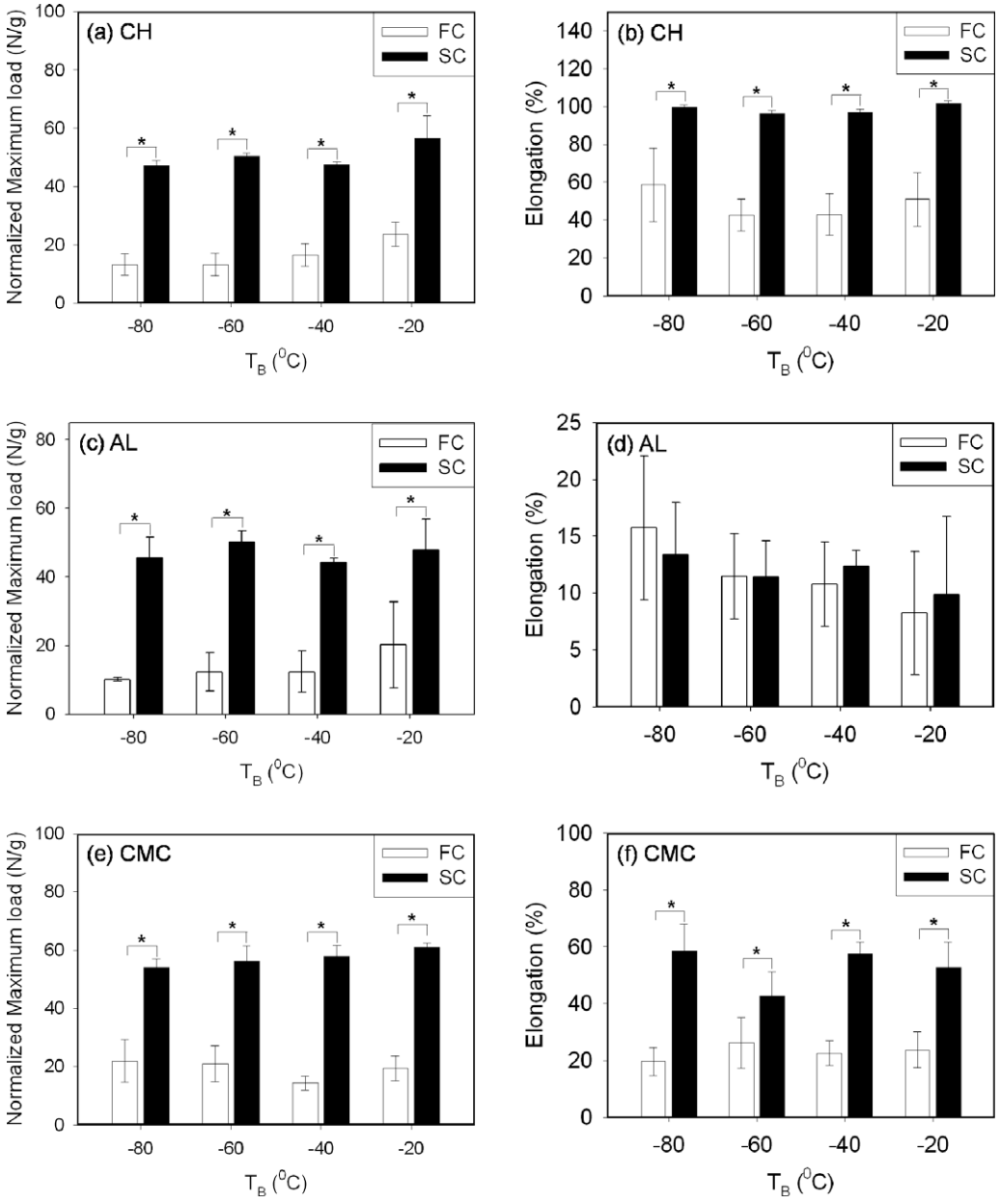

Fig. 5. Mechanical properties of scaffolds prepared with the fast-cooling (FC) and slow-cooling (SC) modes with various T_B values (−20, −40, −60, and −80 °C). (a), (c), and (e) are the normalized tensile strength (maximum load divided by weight of scaffold) and (b), (d), and (f) are the elongation (percentage of strain at maximum load) of the scaffolds ((a and b) for CH, (c and d) for AL, (e and f) for CMC). ($N \geqslant 10$, mean ± SD, $^*p < .05$).

significant difference between the AL scaffolds prepared using these two modes.

However, different T_B values for the FC mode affected the rate of cooling (see Table 1) and induced different ice nucleation and solidification processes. Therefore, different pore structures and material/pore arrangements developed. For the FC mode, there was no difference among the elongation extents of the CH (Fig. 5b), AL (Fig. 5d), and CMC scaffolds (Fig. 5f), but the tensile strength slightly increased with an increase in the T_B. In the SC mode, the use of different T_B values had no significant effect on either the tensile strength or elongation.

From the X-ray diffraction (XRD) analyses, cooling modes had no effect on the semi-crystallization of CH or CMC generated by immersion in the non-solvent (NaOH/ethanol or HCl/ethanol aqueous solution). The XRD patterns of AL showed that it was a more-amorphous polymer than CH or CMC, and the cooling mode had no effect on the AL scaffolds. Taking the mechanical properties, SEM images, and XRD analyses into account, because the direction of tensile force used in determining the mechanical properties of the scaffolds was perpendicular to the direction of stratiform structure of the polysaccharide scaffolds, lower tensile strengths were found for scaffolds prepared by the FC mode.

4. Conclusions

This investigation has shown that the pore space in the scaffolds was mainly created by the formation of ice crystals. SEM and optical microscope images showed that scaffolds with stratiform structures were obtained using the FC mode, because directional freezing and non-simultaneous ice nucleation were induced by the large temperature gradients in the FC mode. In contrast, simultaneous ice nucleation and isotropic pore structures of scaffolds were obtained using the SC mode. Moreover, different pore structures of scaffolds influenced their mechanical properties. Our results show that the normalized tensile strength of scaffolds prepared using the SC mode was approximately three times greater than that prepared using the FC mode. Our results suggest that the cooling mode in the freeze-gelation method is a dominant factor affecting the microstructures and mechanical properties of CH, AL, and CMC scaffolds. Therefore, pore structures can be adjusted via different cooling modes in order to manufacture suitable scaffolds for various tissue engineering applications.

Acknowledgments

This study was financially supported by the Center-of-Excellence Program on Membrane Technology, Ministry of Education, Taiwan and the National Science Council, Taiwan (NSC97-2221-E-002-023-MY2).

References

Berry, C. C., Campbell, G., Spadiccino, A., Robertson, M., & Curtis, A. S. (2004). The influence of microscale topography on fibroblast attachment and motility. *Biomaterials, 25*, 5781–5788.

Bigg, E. K. (1953). The supercooling of water. *Proceedings of the Physical Society of London Section B, 66*, 688–694.

Budiaman, E. R., & Fennema, O. (1987). Linear rate of water crystallization as influenced by temperature of hydrocolloid suspensions. *Journal of Dairy Science, 70*, 534–546.

Capitania, D., Porrob, F., & Segre, A. L. (2000). High field NMR analysis of the degree of substitution in carboxymethyl cellulose sodium salt. *Carbohydrate Polymers, 42*, 283–286.

Chen, S. L., & Lee, T. S. (1998). A study of supercooling phenomenon and freezing probability of water inside horizontal cylinders. *International Journal of Heat and Mass Transfer, 41*, 769–783.

Dong, J. M., & Leong, K. W. (2006). Natural polymers for gene delivery and tissue engineering. *Advanced Drug Delivery Reviews, 58*, 487–499.

Faroongsarng, D., & Sukonrat, P. (2008). Thermal behavior of water in the selected starch- and cellulose-based polymeric hydrogels. *International Journal of Pharmaceutics, 352*, 152–158.

George, M., & Abraham, T. E. (2006). Polyionic hydrocolloids for the intestinal delivery of protein drugs: Alginate and chitosan – A review. *Journal of Controlled Release, 114*, 1–14.

Gokhale, N. R. (1964). Dependence of freezing temperature of supercooled water drops on rate of cooling. *Journal of the Atmospheric Sciences, 22*, 212–216.

Guzman, J. J. M., & Braga, S. L. (2005). Supercooling water in cylindrical capsules. *International Journal of Thermophysics, 26*, 1781–1802.

Ho, M. H., Kuo, P. Y., Hsieh, H. J., Hsien, T. Y., Hou, L. T., Lai, J. Y., et al. (2004). Preparation of porous scaffolds by using freeze-extraction and freeze-gelation methods. *Biomaterials, 25*, 129–138.

Hollister, S. J. (2005). Porous scaffold design for tissue engineering. *Nature Materials, 4*, 518–524.

Hsieh, C. Y., Tsai, S. P., Ho, M. H., Wang, D. M., Liu, C. E., Hsieh, C. H., et al. (2007). Analysis of freeze-gelation and cross-linking processes for preparing porous chitosan scaffolds. *Carbohydrate Polymers, 67*, 124–132.

Kim, I. Y., Seo, S. J., Moon, H. S., Yoo, M. K., Park, I. Y., Kim, B. C., et al. (2008). Chitosan and its derivatives for tissue engineering applications. *Biotechnology Advances, 26*, 1–21.

Kokini, J. L., & Surmay, K. (1994). Steady shear viscosity first normal stress difference and recoverable strain in carboxymethyl cellulose, sodium alginate and guar gum. *Carbohydrate Polymers, 23*, 27–33.

Koop, T., Luo, B., Tsias, A., & Peter, T. (2000). Water activity as the determinant for homogeneous ice nucleation in aqueous solutions. *Nature, 406*, 611–614.

Kuo, Y. C., & Ku, I. N. (2007). Effects of gel concentration, human fibronectin, and cation supplement on the tissue-engineered cartilage. *Biotechnology Progress, 23*, 238–245.

Ma, L., Gao, C., Mao, Z., Zhou, J., Shen, J., Hu, X., et al. (2003). Collagen/chitosan porous scaffolds with improved biostability for skin tissue engineering. *Biomaterials, 24*, 4833–4841.

Moshfeghian, A., Tillman, J., & Madihally, S. V. (2006). Characterization of emulsified chitosan–PLGA matrices formed using controlled-rate freezing and lyophilization technique. *Journal of Biomedical Materials Research Part A, 79*, 418–430.

Muschler, G. F., Nakamoto, C., & Griffith, L. G. (2004). Engineering principles of clinical cell-based tissue engineering. *Journal of Bone and Joint Surgery – American Volume, 86*, 1541–1558.

Muzzarelli, R. A. A., Baldassarre, V., Conti, F., Ferrara, P., Biagini, G., Gazzanelli, G., et al. (1988). Biological activity of chitosan: Ultrastructural study. *Biomaterials, 9*, 247–252.

Nam, Y. S., & Park, T. G. (1999). Porous biodegradable polymeric scaffolds prepared by thermally induced phase separation. *Journal of Biomedical Materials Research, 47*, 8–17.

O'Brien, F. J., Harley, B. A., Yannas, I. V., & Gibson, L. (2004). Influence of freezing rate on pore structure in freeze-dried collagen-GAG scaffolds. *Biomaterials, 25*, 1077–1086.

Okawa, S., Saito, A., & Suto, H. (2002). The experimental study on freezing of supercooled water using metallic surface. *International Journal of Refrigeration – Revue Internationale Du Froid, 25*, 514–520.

Perkyns, J., & Pettitt, B. M. (1996). Dependence of hydration free energy on solute size. *Journal of Physical Chemistry, 100*, 1323–1329.

Rezwan, K., Chen, Q. Z., Blaker, J. J., & Boccaccini, A. R. (2006). Biodegradable and bioactive porous polymer/inorganic composite scaffolds for bone tissue engineering. *Biomaterials, 27*, 3413–3431.

Searles, J. A., Carpenter, J. F., & Randolph, T. W. (2001). The ice nucleation temperature determines the primary drying rate of lyophilization for samples frozen on a temperature-controlled shelf. *Journal of Pharmaceutical Sciences, 90*, 860–871.

Thomson, R. C., Mikos, A. G., Beahm, E., Lemon, J. C., Satterfield, W. C., Aufdemorte, T. B., et al. (1999). Guided tissue fabrication from periosteum using preformed biodegradable polymer scaffolds. *Biomaterials, 20*, 2007–2018.

Wang, Y. C., Kao, S. H., & Hsieh, H. J. (2003). A chemical surface modification of chitosan by glycoconjugates to enhance the cell–biomaterial interaction. *Biomacromolecules, 4*, 224–231.

Whang, K., Thomas, C. H., Healy, K. E., & Nuber, G. (1995). A novel method to fabricate bioabsorbable scaffolds. *Polymer, 36*, 837–842.

Wood, G. R., & Walton, A. G. (1970). Homogeneous nucleation kinetics of ice from water. *Journal of Applied Physics, 41*, 3027–3036.

Yoon, J. I., Moon, C. G., Kim, E., Son, Y. S., Kim, J. D., & Kato, T. (2001). Experimental study on freezing of water with supercooled region in a horizontal cylinder. *Applied Thermal Engineering, 21*, 657–668.

Zeltinger, J., Sherwood, J. K., Graham, D. A., Müeller, R., & Griffith, L. G. (2001). Effect of pore size and void fraction on cellular adhesion, proliferation, and matrix deposition. *Tissue Engineering, 7*, 557–572.

Zhang, H., Hussain, I., Brust, M., Butler, M. F., Rannard, S. P., & Cooper, A. I. (2005). Aligned two- and three-dimensional structures by directional freezing of polymers and nanoparticles. *Nature Materials, 4*, 787–793.